Chemosphere 319 (2023) 137972

Contents lists available at ScienceDirect

Chemosphere

journal homepage: www.elsevier.com/locate/chemosphere

Photoinduced production of substances with humic-like fluorescence, upon irradiation of water samples from alpine lakes

Luca Carena [a], Yiqun Wang [b], Sasho Gligorovski [b,**], Silvia Berto [a], Stéphane Mounier [c], Davide Vione [a,*]

[a] Dipartimento di Chimica, Università di Torino, Via Pietro Giuria 5, 10125, Torino, Italy
[b] State Key Laboratory of Organic Geochemistry, Guangzhou Institute of Geochemistry, Chinese Academy of Sciences, Guangzhou, 510 640, China
[c] Univ. Toulon, Aix Marseille Univ., CNRS/INSU, IRD, MIO UM 110, Mediterranean Institute of Oceanography, CS 60584, 83041, Toulon, France

HIGHLIGHTS

- Compounds with humic-like fluorescence were formed upon lake-water irradiation.
- Increase in water absorbance upon irradiation was also observed.
- Humic-poor water samples were taken from mountain lakes in late summer.
- Protein and humic components were detected by PARAFAC analysis.

GRAPHICAL ABSTRACT

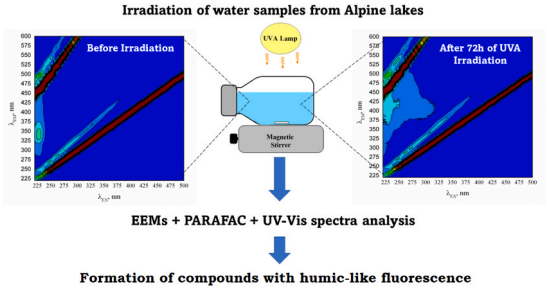

ARTICLE INFO

Handling Editor: Willie Peijnenburg

Keywords:
Aquagenic organic matter
Photochemistry
Fluorescence
PARAFAC analysis
Spectral slope

ABSTRACT

Evidence is here provided that irradiation of some lake water samples can trigger the formation of fluorophores with humic-like properties, at the same time increasing water absorbance. This phenomenon is the opposite of photobleaching, which is often observed when natural waters are irradiated. The photoproduced humic-like fluorophores observed here would be of autochthonous rather than allochthonous origin, which marks a difference with the fraction of humic substances that derives from terrestrial sources. Photogeneration of humic-like compounds can be highlighted in water samples where the fluorescence signal of initially occurring humic substances is low, so that their photobleaching is minimised. Samples that are most likely to show photoinduced formation of humic-like fluorophores are in fact characterised by high values of protein-like vs. humic-like contribution ratios to fluorescence, as evidenced by parallel factor (PARAFAC) analysis. Mountain lakes in late summer appear to be suitable candidates to highlight the described phenomenon. In some cases, lake-water irradiation caused a decrease in the spectral slope of the absorbance that, together with increasing absorbance values, is consistent with an increase in molecular mass and aromaticity of organic matter. The absorbance increase triggered by irradiation might play a role in screening biologically harmful UV radiation, in mountain environments that would otherwise be characterised by very clear water that allows for easy transmission of UV light along the water column.

* Corresponding author.
** Corresponding author.
E-mail addresses: gligorovski@gig.ac.cn (S. Gligorovski), davide.vione@unito.it (D. Vione).

https://doi.org/10.1016/j.chemosphere.2023.137972
Received 30 November 2022; Received in revised form 24 January 2023; Accepted 25 January 2023
Available online 27 January 2023

1. Introduction

Humic substances (HS) are important components of both chromophoric and fluorescent dissolved organic matter (respectively, CDOM and FDOM) in natural waters, and play important roles as metal complexing agents, radiation absorbers, and photosensitisers (Krachler and Krachler, 2021; Nelson and Siegel, 2013; Zhou et al., 2019). Interaction between HS and metals or hydrophobic pollutants contributes to keep these species dissolved, and to change their toxicity or bioavailability (De Paolis and Kukkonen, 1997; Koukal et al., 2003; Suzuki and Shoji, 2020; Worms et al., 2015). Furthermore, HS screen sunlight and they are a key factor in, among others, light penetration in the water column, thermocline depth in stratified lakes, protection of living organisms against harmful UV radiation, and contaminant degradation *via* photochemically produced reactive intermediates (Berg et al., 2019; Remucal, 2014; Shank et al., 2010; Sommaruga, 2001; Sommaruga et al., 1999; Vione et al., 2014). Spectroscopic techniques (both absorption and fluorescence) are widely used for HS detection and characterisation (Coble, 1996; Galgani et al., 2011; Loiselle et al., 2009).

A major route of HS to surface waters is leaching from soil, in which case HS make up an important fraction of allochthonous organic matter (Osburn and Stedmon, 2011). Precipitation water plays key role in transferring soil HS to water basins (Nguyen et al., 2013; Tipping et al., 1999), where HS can for instance undergo photobleaching upon exposure to sunlight (Brinkmann et al., 2003; Del Vecchio and Blough, 2002; Helms et al., 2014). Photobleaching is the loss of chromophores (and often also the fluorophores) induced by sunlight radiation, and it can be a very important transformation route for biorecalcitrant compounds like HS (Clark et al., 2019; Gu et al., 2017; Niu et al., 2014; Vähätalo and Wetzel, 2004).

The scenario is actually more complex, because HS are partially aquagenic. This means they can be formed autochthonously in natural surface waters, from a range of precursors. Recent evidence suggests that a complex network of biological and photoinduced processes may be responsible for the production and processing of fluorescent organic matter, starting from extracellular polymeric substances released by microorganisms (Fox et al., 2019; Yang et al., 2021). Aquagenic HS take part in these processes, where they are both produced and consumed (He et al., 2016; Yang et al., 2021), and where the exact roles of radiation and biological reactions are still unclear.

On the one side, photobleaching is a well-known, radiation-induced phenomenon involving HS (Dainard et al., 2015; Del Vecchio and Blough, 2002; Helms et al., 2008; Yamashita et al., 2013). On the other side, laboratory evidence suggests that compounds with HS-like properties, including HS-like fluorescence, are produced by irradiation of precursors such as amino acids (tryptophan and tyrosine) and phenols, including lignin breakdown compounds (Berto et al., 2016, 2018; Bianco et al., 2014). Photoinduced formation of humic-like substances has opposite features compared with photobleaching, because it causes an increase in long-wavelength (>300 nm) absorbance. From a mechanistic point of view, this photochemical process could involve dimerisation/oligomerisation, as well as hydroxylation of the precursor molecules (see Scheme S1 in the Supplementary Material, hereinafter SM, for a possible example of such processes) (De Laurentiis et al., 2013; Hoffer et al., 2004; Mabato et al., 2022). Indeed, evidence suggests that phenolic oligomers and poly-hydroxylated aromatic compounds are reasonable humic fluorophores (Vione et al., 2021).

Unfortunately, very little is currently known about the possibility that formation of HS (or otherwise, of compounds with HS-like fluorescence) may occur photochemically in real surface-water samples. The main obstacle to highlight this process is the fact that existing HS in the sample would undergo photobleaching, thereby potentially masking possible photoinduced formation of additional HS-like compounds from non-humic precursors. Because of this problem, the ideal sample to be irradiated should initially contain little to no HS, which is not easy to be attained. However, past studies have found out that water from mountain lakes at the end of the boreal summer season (mid September) exhibits fluorescence signals that can be assigned to proteins, or even to sunlight-absorbing plankton pigments, but little to no HS fluorescence (De Laurentiis et al., 2012). In contrast, HS signals are detected in samples taken from the same lakes, soon after ice melting (mid June) (Bianco et al., 2014). Possible reasons for this finding are summer (June–August) photobleaching of initially-occurring HS, plus high turnover of algal cells in late summer, including important cell lysis.

Excitation-emission matrix (EEM) fluorescence spectroscopy is one of the most straightforward ways to characterise organic matter in natural water samples (Minor et al., 2014; Stedmon et al., 2003). The signals that are most often detected in EEM spectra are those of proteins and HS (Vione et al., 2021). Protein fluorescence is detected based on the main fluorophores, *i.e.* tyrosine (Ex ~ 230 nm; Em ~ 300 nm, where Ex means excitation wavelength and Em means emission wavelength), and tryptophan (Ex ~ 230 nm; Em ~ 350 nm) (Coble, 1996; Stedmon

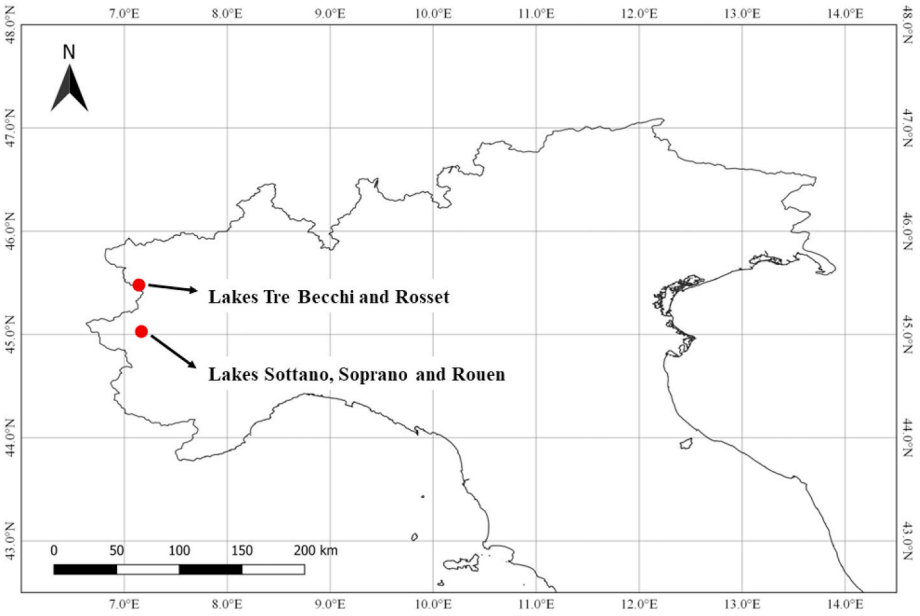

Fig. 1. Map showing the location of the lakes under study (Piedmont region, NW Italy).

et al., 2003; Trubetskaya et al., 2016). In contrast, HS typically have two fluorescence peaks at Ex/Em = ~250/~450 nm, and ~320/~450 nm (Bridgeman et al., 2011; Coble, 1996; Stedmon et al., 2003). The presence of multiple signals in the EEM spectrum of a natural water sample may require the use of decomposition techniques to separate the different components, among which PARAllel FACtor analysis (PARAFAC), introduced by Bro (1997) and popularised by Stedmon et al. (2003), plays a major role. Indeed, spectral fluorescence data are multi-way (three-way) signals that depend on the wavelength of light absorbed (excitation) and the wavelength at which fluorescence is observed (emission). These data enter in a data cube that the PARAFAC algorithm fits by minimising the difference between the three-way model parameters (emission, excitation, and contribution) and the observed signals that constitute the Excitation-Emission Matrices of fluorescence (EEMs) (Andersen and Bro, 2003; Cory and McKnight, 2005; Murphy et al., 2013).

In this context, this work has the goal of figuring out if compounds with humic-like fluorescence can actually be formed upon irradiation of samples of natural surface water. To minimise the occurrence of humic fluorescence signals in the initial samples, the latter were taken from mountain lakes in late summer. EEM spectroscopy, coupled with PARAFAC analysis, was mainly used to monitor changes in fluorescent organic matter in the investigated samples.

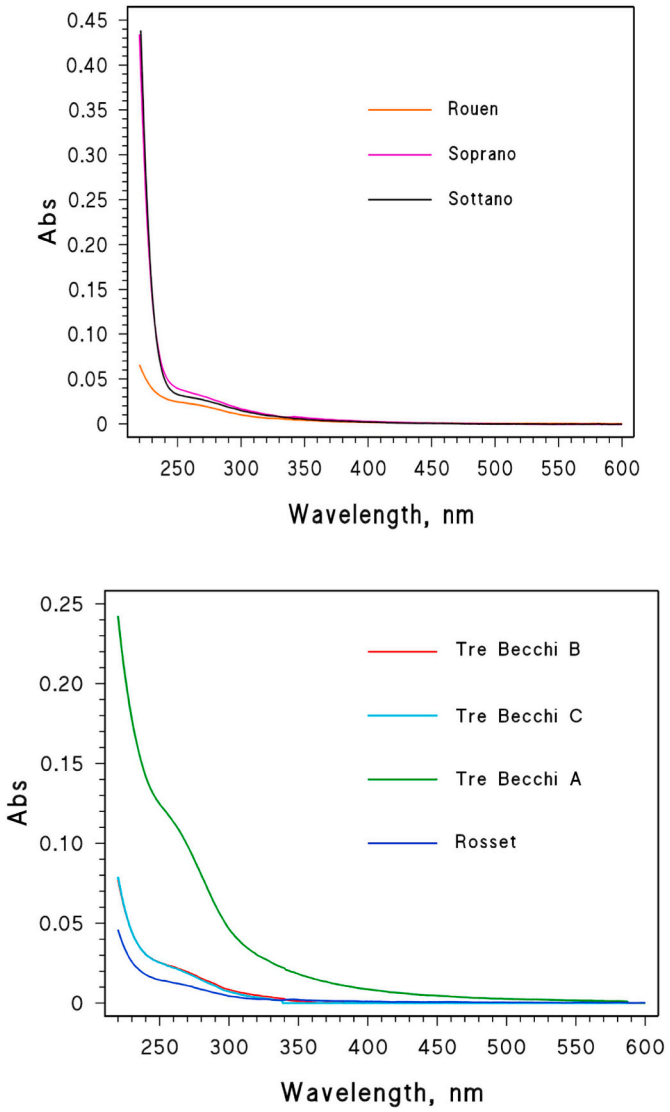

Fig. 2. Absorption spectra (optical path length b = 5 cm) of the lake water samples under study.

2. Materials and methods

2.1. Alpine lakes under study

The study lakes are located in the north-western part of the Italian Alps, in the Piedmont region (see map in Fig. 1). In particular, Lakes Rouen, Soprano, and Sottano are located in the Orsiera-Rocciavrè Natural Park, at 2391, 2213, and 2102 m a.s.l., respectively, while Lake Rosset (2701 m a.s.l.) and the three Lakes Tre Becchi (2727 m a.s.l., hereinafter called Tre Becchi A, B, and C [A = Left; B=Central; C = Right]) are in the Gran Paradiso National Park. The lakes are small and shallow, all located above the tree line, and mainly surrounded by rocks and grasses. During sampling (mid-September 2018, *i.e.*, late boreal summer) the surface of the lakes was completely ice-free.

Water samples (1 L from each lake) were kept refrigerated and in the dark during transport to the laboratory, where they were vacuum-filtered with polyamide filters (0.45 μm pore size, Sartorius). In order to minimise modifications caused by residual biological activity, the filtered samples were kept in the dark at ~5 °C till further processing. The lake water samples were first characterised for dissolved organic carbon (DOC), inorganic carbon (IC), and pH (see Table S1 in the Supplementary Material, hereinafter SM). The DOC was obtained as the difference between total carbon and IC, using a Shimadzu TOC-VCSH instrument based on the catalytic combustion method, equipped with an ASI-V autosampler. The pH values were measured with a Metrohm combined glass electrode (code number 6.0233.100).

2.2. Irradiation experiments

Irradiation runs of lake water (80 mL) were carried out in 100 mL Duran®-glass flasks under a Philips TL K05 lamp, and irradiation was mainly from the top. This lamp emits most radiation in the wavelength range of 300–500 nm, with a broad band emission in the UVA region (maximum at 365 nm). The lamp choice is motivated by the fact that UVA is the main component of sunlight UV, and that a very important fraction of sunlight absorption (as absorbed photon flux density) by chromophoric organic material is observed in the UVA range (Wolf et al., 2018).

At different irradiation times (between 7 and 72 h), 5-mL or 10-mL aliquots of lake water were withdrawn for immediate EEM or UV–Vis characterisation, respectively. Each flask (80 mL of lake water) was sampled for a maximum of two times, in order not to affect too much the irradiated solution optical path (3 cm). Therefore, each series of EEM or UV–Vis spectra referred to a given lake was obtained by independent irradiation of at least two separate aliquots of the same sample.

The spectral photon flux density of the lamp ($p^{\circ}(\lambda)$, see Fig. S1 in the SM) was obtained by combination of two techniques: *(i)* wavelength-resolved lamp emission measurements, with a calibrated Ocean Optics USB 2000 CCD spectrophotometer, and *(ii)* chemical actinometry, based on 2-nitrobenzaldehyde (2NBA) (Galbavy et al., 2010; Willett and Hites, 2000).

CCD measurement yields the raw lamp spectrum $i^{\circ}(\lambda)$ on a moles-of-photons basis, which is proportional to the spectral photon flux density $p^{\circ}(\lambda) = \vartheta\, i^{\circ}(\lambda)$, where ϑ is the proportionality factor, and $p^{\circ}(\lambda)$ has units of Einstein L^{-1} s^{-1} nm^{-1}. Actinometry yields the moles of photons (Einstein units) that pass through the solution per unit volume and time, taking into account the possible reflection/scattering processes at the different interfaces (for instance, air-glass, air-water, or glass-water) (Galbavy et al., 2010). The degradation rate of 2NBA (R_{2NBA}, units of mol L^{-1} s^{-1}) can be described as follows:

$$R_{2NBA} = \Phi_{2NBA} P_{a,2NBA} = \Phi_{2NBA} \int_{\lambda} p^{\circ}(\lambda)\left[1 - 10^{-A(\lambda)}\right] d\lambda \quad (1)$$

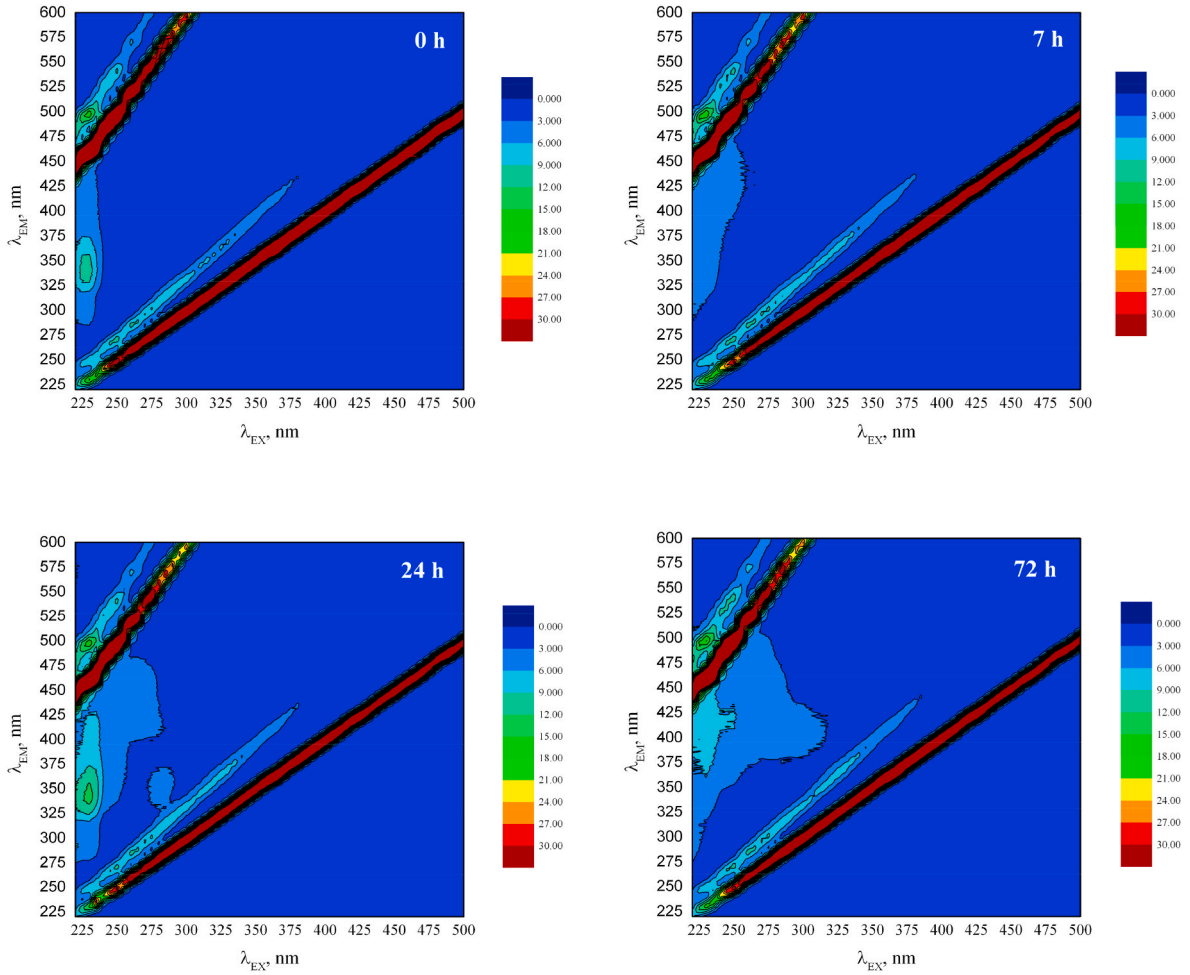

Fig. 3. Trends of the EEM fluorescence spectra of water sampled from Lake Tre Becchi B, as a function of the irradiation time. EEM signals were normalised for the quinine sulphate unit.

where $\Phi_{2NBA} = 0.4$ mol Einstein^{-1} is the photolysis quantum yield of 2NBA (Galbavy et al., 2010), $P_{a,2NBA}$ [Einstein L^{-1} s^{-1}] the photon flux absorbed by 2NBA, and $A(\lambda)$ [unitless] the absorbance of the irradiated solution. On this basis, the factor ϑ can be obtained from known values, as follows (Carena et al., 2019):

$$\vartheta = \frac{R_{2NBA}}{\Phi_{2NBA} \int_{\lambda} i^{\circ}(\lambda)\left[1 - 10^{-A(\lambda)}\right] d\lambda} \quad (2)$$

To measure R_{2NBA}, aqueous solutions of 2NBA (80 mL, 80 μmol L^{-1} initial concentration) were irradiated under the lamp, and sampled (1.2 mL) after 0.5, 1, 2, 3, and 4 min. The 2NBA concentration was quantified by means of liquid chromatography (HPLC-DAD instrument; Carena et al., 2019). Then, R_{2NBA} was obtained from the 2NBA time trend, by means of the initial slope method.

2.3. EEM and UV–vis measurements

The fluorescence excitation−emission matrix (EEM) spectra were measured with a Cary Eclipse fluorescence spectrofluorimeter, using 1-cm fluorescence quartz cuvettes. Excitation wavelengths scan was from 220 till 500 nm, with 5 nm increment steps, while emission signals were taken from 220 till 600 nm, with 1 nm steps. Slit width was 10 nm on both excitation and emission. EEM signals were normalised for the quinine sulphate unit (QSU; Fox et al., 2017). The QSU was measured from the fluorescence signal emitted at 451 nm by an acidic quinine sulphate (QS) aqueous solution (4 μg L^{-1} QS + 0.1 N H_2SO_4), after excitation at 350 nm (Fox et al., 2019).

The UV–Vis absorption spectra of the alpine lake water samples were measured with a V-550 Jasco spectrophotometer, using 5.0 cm optical path quartz cuvettes (Hellma). The absorption spectra thus obtained are reported in Fig. 2. In some cases, absorption spectra were also measured of irradiated lake water samples, and the spectral slope S was calculated as a function of the irradiation time. To do so, the 300–345 nm spectral interval was considered for the absorption spectra, because the relevant data were well described by an exponential function (**Eq. (3)**; absorbance above 345 nm was often negligible, and absorbance below 300 nm was often non-exponential, see Fig. 2):

$$A(\lambda) = A_o e^{-s\lambda} \quad (3)$$

In **Eq. (3)**, $A(\lambda)$ is the absorbance at the wavelength λ, A_o is the pre-exponential term, and S is the spectral slope (Helms et al., 2008; Loiselle et al., 2009; Sharpless and Blough, 2014). The value of S was obtained by a linear least-square fit procedure of ln [$A(\lambda)$] *vs.* λ data, with A_o and S as free-floating variables.

2.4. PARAFAC analysis

The PARAFAC analysis of the EEM spectra was carried out with the Progmeef software (*http://protee.univ-tln.fr/PROGMEEF.html*), with preliminary elimination of the Rayleigh and Raman scattering signals, using Zepp's method (Zepp et al., 2004). The low absorbance values of the samples (see Fig. 2) made inner-filter correction unnecessary. PARAFAC was applied to all the initial (irradiation time $t = 0$) EEM

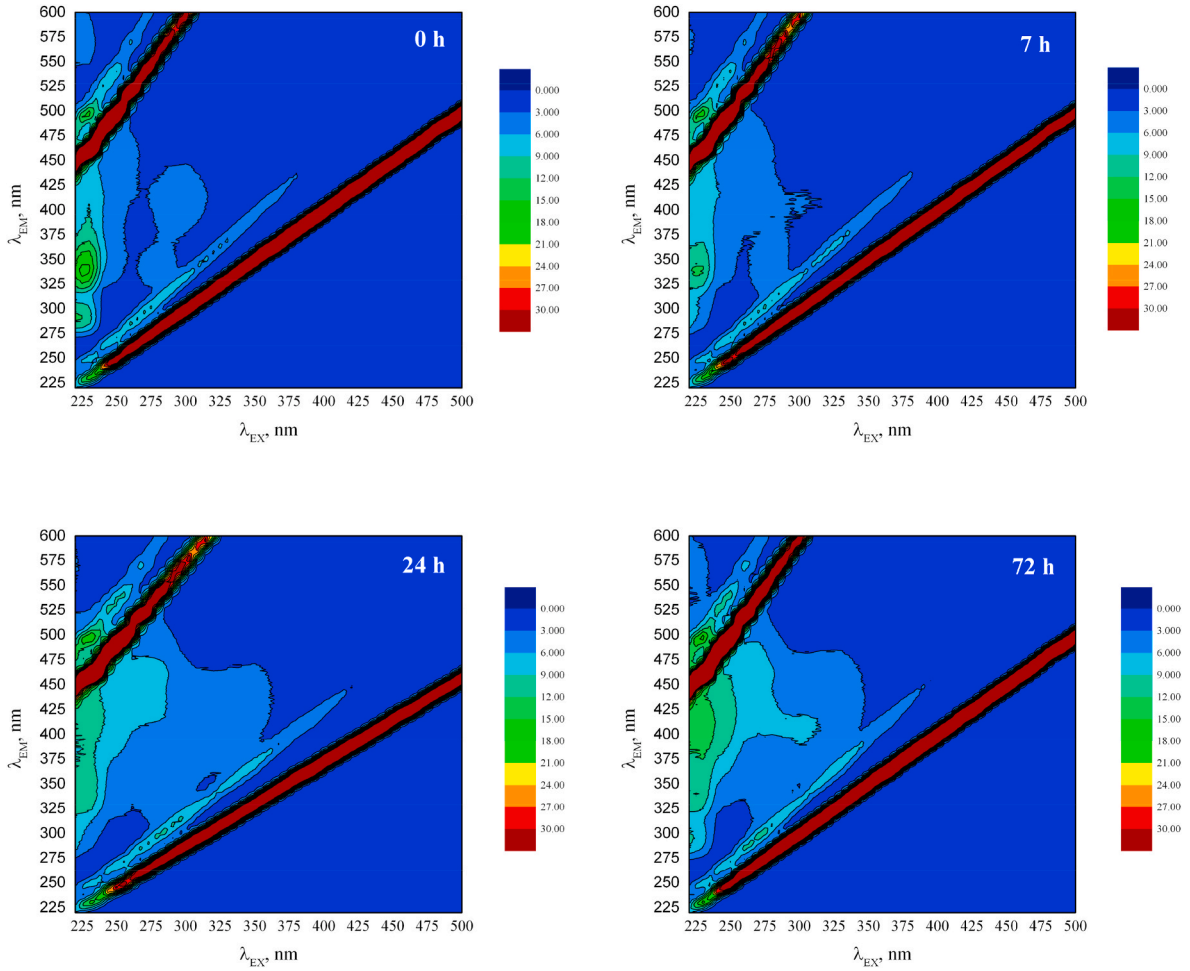

Fig. 4. Trends of the EEM fluorescence spectra of water sampled from Lake Soprano, as a function of the irradiation time. EEM signals were normalised for the quinine sulphate unit.

spectra of the different lake water samples and, for every lake taken separately, also to each series of irradiation times (from 0 to 72 h). A range of 2–4 components was initially set, and the maximum number of components ensuring a CONCORDIA score >70% was chosen. In all the cases, a three-component model proved suitable to reproduce sample fluorescence.

2.5. Irradiation experiments coupled with FT-ICR MS measurements

Separate solutions of tyrosine or tryptophan (each at 0.1 mM initial concentration) were irradiated in a Pyrex glass photoreactor (130 mL volume), equipped with a 500 W Xenon lamp (Wang et al., 2022b). The mass spectrometric measurements (FT-ICR MS: Fourier Transform-Ion Cyclotron Resonance Mass Spectrometry) of the irradiated samples, taken every 2 h, were carried out with a Bruker 9.4 T solariX instrument (100–800 Da mass range; average mass resolution about 350,000 was estimated at *m/z* 319), equipped with an electro-spray ionisation (ESI) interface that was operated in negative ion mode. Further experimental details are reported as Supplementary Material, **Text S1**.

Aromaticity equivalent (*Xc*) and double-bond equivalent (DBE) values were used to get insight into photodegradation product distribution. The DBE values were calculated based on **Eq. (4)**, for the elemental composition $C_cH_hO_oN_n$ obtained by FT-ICR MS (Kourtchev et al., 2016):

$$DBE = c - \frac{h}{2} + \frac{n}{2} + 1 \quad (4)$$

where *c*, *h*, *o*, and *n* correspond to the number of carbon, hydrogen, oxygen, and nitrogen atoms in the neutral formula, respectively.

The value of *Xc*, which is used to identify aromatic and polyaromatic structures in a complex mixture of compounds, was calculated as follows (Yassine et al., 2014):

$$Xc = \frac{2C + N - H - 2mO}{DBE - mO} + 1 \quad (5)$$

If DBE $\leq m\,O$, or $Xc \leq 0$, it was taken $Xc = 0$, where *m* is the fraction of O atoms in π-bond structures of a compound. Because of the interest in amino acid, and because ESI is sensitive to functional groups such as, for instance, carboxylic acid (R–COOH) and ester (R-$COOR_1$), we used $m = 0.5$ for the calculation of the *Xc* value in this study (Wang et al., 2022a, 2021; Yassine et al., 2014).

Reconstructed mass spectra were normalised to the intensity of the tyrosine (m/z = 180.0667) and tryptophan (m/z = 203.0826) peaks, respectively. All the formulae of the compounds were written in their neutral form to avoid confusion.

3. Results and discussion

3.1. Time evolution of lake-water samples upon irradiation: EEM spectra

EEM spectra of the lake water samples were measured at different irradiation times. The fluorescence signals of the lake water evolved upon irradiation, coherently with the fact that the studied samples all showed non-negligible absorption in the UVA region (see Fig. 2). In

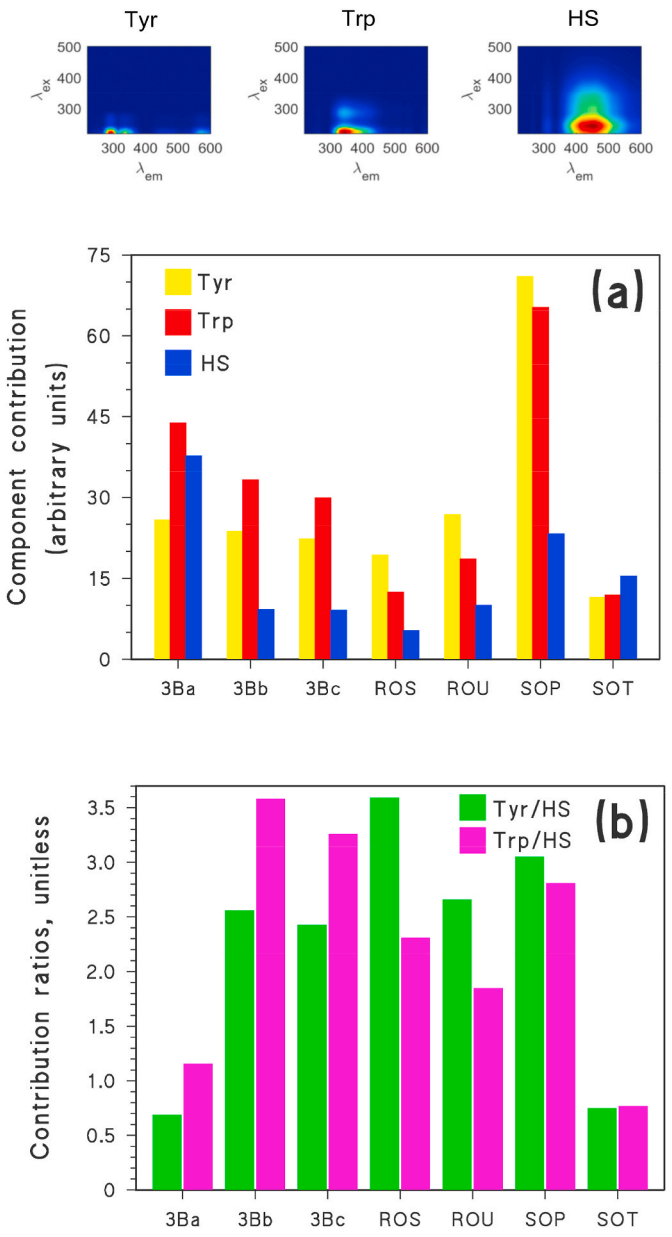

Fig. 5. (a) Contributions (arbitrary units) of the three fluorescence components, found by PARAFAC analysis of the EEM spectra of the investigated lake-water samples before irradiation. Component acronyms: Tyr = tyrosine-like component; Trp = tryptophan-like; HS = humic-like. The EEM traces of the three components are shown in the upper figure panel. Lake acronyms: 3Ba = Tre Becchi A; 3Bb = Tre Becchi B; 3Bc = Tre Becchi C; ROS = Rosset; ROU = Rouen; SOP = Soprano; SOT = Sottano. **(b)** Component contribution ratios, Tyr/HS (left-side bars) and Trp/HS (right-side bars), in the investigated lake-water samples.

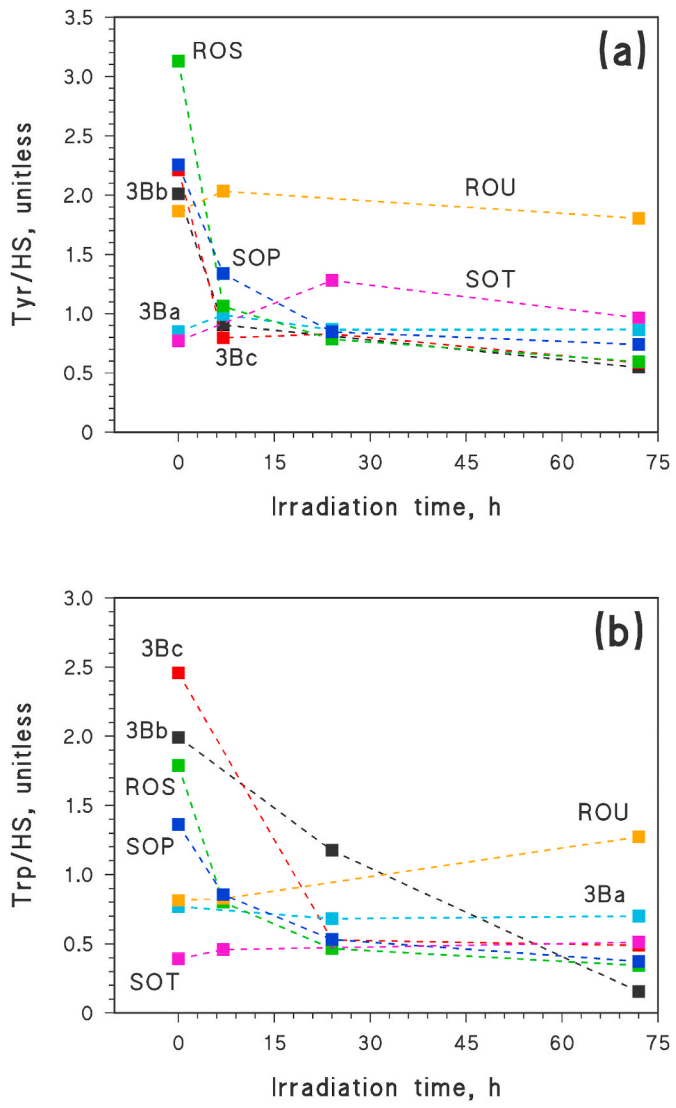

Fig. 6. Time trend of the PARAFAC contribution ratios Tyr/HS **(a)** and Trp/HS **(b)**, upon UVA irradiation of the lake water samples under study. Lake acronyms: 3Ba = Tre Becchi A; 3Bb = Tre Becchi B; 3Bc = Tre Becchi C; ROS = Rosset; ROU = Rouen; SOP = Soprano; SOT = Sottano.

particular, in the case of the lakes Tre Becchi B (Fig. 3) and Soprano (Fig. 4), some evidence could be seen at first sight of a gradual shift in fluorescence from the protein/phenolic region (emission wavelength λ_{EM} around 325–350 nm; Stedmon et al., 2003) to the humic one (λ_{EM} around 400–450 nm; Stedmon et al., 2003), which points to photoinduced formation of HS-like fluorophores. In the other cases (Tre Becchi A, Tre Becchi C, Rosset, Rouen, Sottano, Figs. S2–S6 in SM) there was often an increase in humic-like fluorescence, without a clear trend of the signals in the protein region.

Control experiments carried out in the dark did not show significant changes in the fluorescence spectra (data not shown), which suggests that any residual biological activity in the filtered lake water samples was not able to affect fluorophores to a significant extent.

3.2. PARAFAC analysis

PARAFAC analysis of the EEM spectra of lake water samples before irradiation showed the presence of three components (see Fig. 5). The first had Ex/Em ~230/300 nm, which is usually assigned to a protein component produced by fluorescence emission of tyrosine. The second component had Ex/Em ~230/350 nm, which is also a protein component produced by fluorescence emission of tryptophan.

The third component had Ex_1/Em_1 ~ 250/450 nm and Ex_2/Em_2 ~ 330/450 nm, which respectively overlap with peaks A and C of humic substances (Coble, 1996). Hereinafter, these three components will be labelled as Tyr, Trp, and HS, respectively.

The PARAFAC contributions can be related to pseudo-concentrations (arbitrary units) and give insight into the fluorescence intensity of each component among the lakes. As shown in Fig. 5a, Lake Soprano (SOP) had the highest Tyr and Trp contributions, which were minimum in Lake Sottano (SOT). Concerning HS, Tre Becchi A (3Ba) was the most impacted lake, followed by SOP.

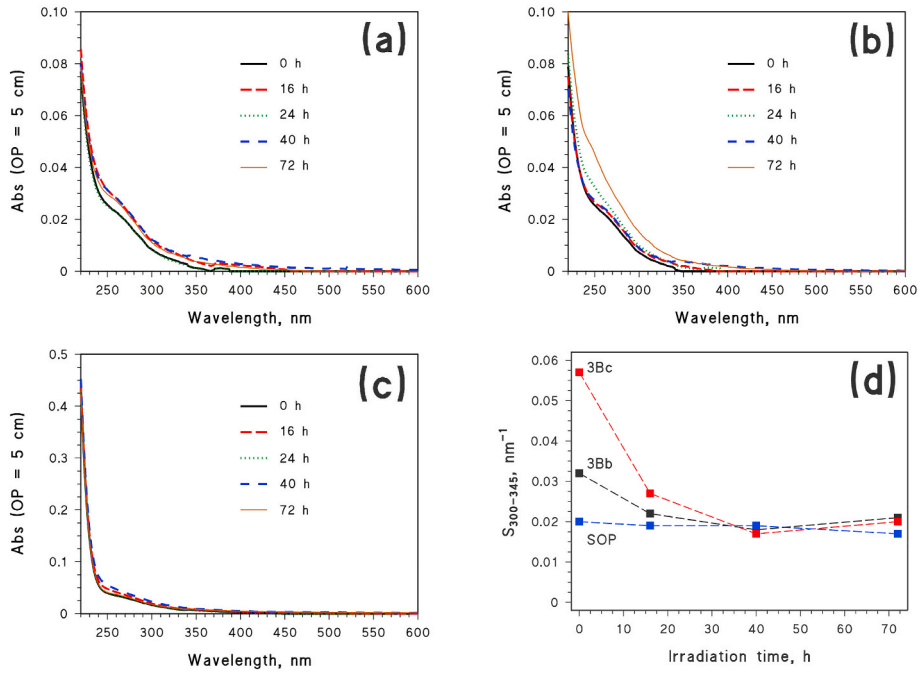

Fig. 7. Trend of the absorbance (measured over an optical path length of 5 cm) as a function of the irradiation time, for the following lake samples: **(a)** Tre Becchi B; **(b)** Tre Becchi C; **(c)** Soprano. **(d)** Time trend of the spectral slope *S* (calculated over the wavelength interval of 300–345 nm) for the three irradiated samples: 3Bb = Tre Becchi B; 3Bc = Tre Becchi C; SOP = Soprano.

Using the Tyr/HS and Trp/HS contribution ratios, one can compare the relative fluorophore contributions under the hypothesis that fluorescence quantum yields are constant between samples. Fig. 5b shows that 3Ba and SOT were the lakes with the lowest Tyr/HS and Trp/HS contribution ratios.

PARAFAC analysis was also applied to time series of EEM spectra, derived from irradiation experiments. In particular, each time series from each irradiated lake-water sample was processed separately, always finding similar components as before (Tyr, Trp, and HS). The time evolution of the component contribution ratios is shown in Fig. 6 (**6a**: Tyr/HS; **6b**: Trp/HS). A decrease of contribution ratio over irradiation time was observed in the case of samples from lakes Rosset (ROS), Soprano (SOP), Tre Becchi B (3Bb), and Tre Becchi C (3Bc), which were also the samples with the highest values of contribution ratios before irradiation. The observed decrease in the Tyr/HS and Trp/HS ratios was largely due to an increase in HS fluorescence contribution, which was apparent in all the samples except for Tre Becchi A (see Fig. S7 in SM). The overall results warrant two observations: *(i)* there is here experimental evidence that HS-like fluorescence can be produced upon irradiation of lake water samples, which in several cases led to a reduction in the Tyr/HS and Trp/HS contribution ratios, and *(ii)* the phenomenon was best observed in samples where initial contribution ratios were high, most likely because low HS contribution to initial fluorescence minimises the impact of photobleaching on HS-like fluorescence signals.

A decrease of Tyr/HS and Trp/HS ratios over time could be consistent with photoinduced transformation of protein-like into HS-like fluorophores (Berto et al., 2016, 2018). However, the same phenomenon might also be explained by different events, such as for instance the transformation of non-fluorescent precursors into HS-like fluorophores, or an increase in fluorescence intensity of already existing fluorophores upon photoprocessing.

To corroborate evidence over the production of HS-like fluorophores, three samples (Tre Becchi B, Tre Becchi C, Soprano) were chosen for additional irradiation experiments, where the absorbance was monitored as a function of irradiation time. As shown in Fig. 7a–c, lake-water absorbance increased upon irradiation, which is the opposite of photobleaching and indicates that photoinduced formation of chromophores took place. Similar findings about increasing absorbance have already been reported in irradiation experiments of synthetic solutions, where formation of compounds with HS-like fluorescence has been observed starting from phenolic or amino-acidic precursors (Bianco et al., 2014; Berto et al., 2016).

The time evolution of the spectral slope *S* was monitored in the same samples. The results reported in Fig. 7d indicate that *S* decreased with irradiation in two out of three cases, *i.e.*, Tre Becchi B and Tre Becchi C. The spectral slope *S* is inversely correlated with the molecular mass of CDOM (Helms et al., 2008) and, in two cases, an increase in lake-water absorbance upon irradiation occurred alongside with a decrease in *S*. No significant *S* decrease was observed in the sample from Lake Soprano (Fig. 7d), which was also the sample showing the slightest variation of absorbance upon irradiation (Fig. 7c). These findings suggest that, in some irradiated lake water samples, increasing absorbance might be associated with an increase in the molecular mass of organic matter.

3.3. Irradiation of model molecules

Additional irradiation experiments were carried out to see if similar phenomena could occur in the presence of amino-acidic precursors. In particular, irradiation of tryptophan and tyrosine has already been shown to produce compounds with HS-like fluorescence (Bianco et al., 2014). Fig. 8 reports the results of FT-ICR MS measurements of irradiated tryptophan solutions, which shows the following: *(i)* The photodegradation of tryptophan produced compounds with both higher and lower molecular mass, compared to the parent molecule (Fig. 8a). In particular, for irradiation times > 2 h, ~30% of the detected signals could be attributed to polyaromatic compounds (*i.e.*, compounds having more than one aromatic ring, Xc > 2.7) (Liu et al., 2020; Loisel et al., 2021; Mekic et al., 2020; Wang et al., 2022a). Therefore, alongside with fragmentation, formation of larger structures was operational. *(ii)* The absorbance of the irradiated solution at $\lambda > 300$ nm increased with irradiation. *(iii)* The value of *S* between 290 and 310 nm decreased with irradiation (Fig. 8b).

Based on literature reports, formation of compounds with higher molecular mass is the most likely reason of the observed spectral

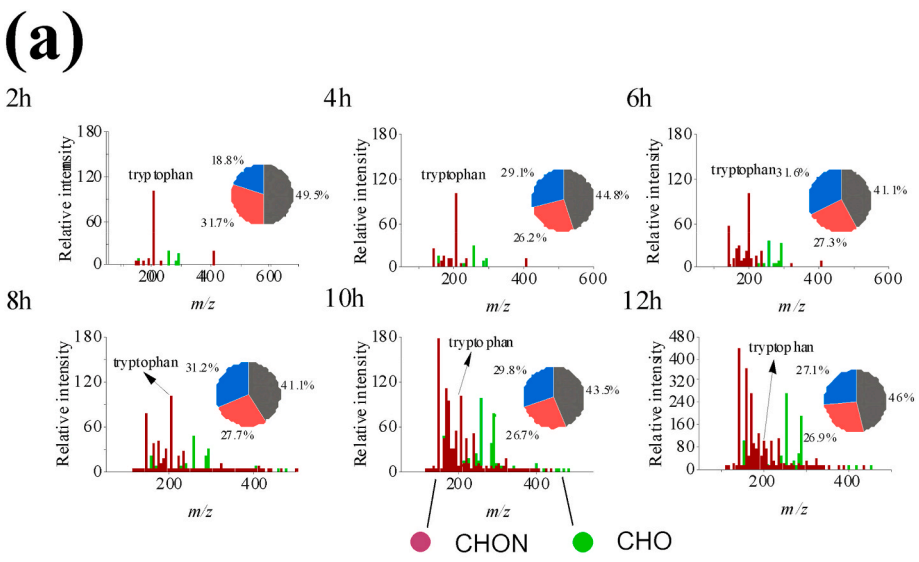

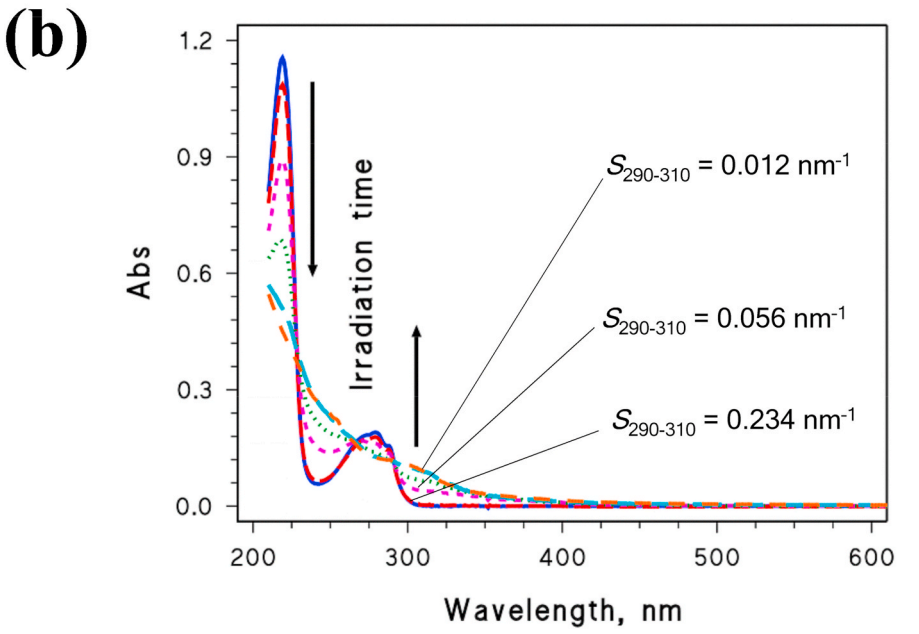

Fig. 8. (a) Reconstructed mass spectra of 0–12 h photo-degradation of 0.1 mM tryptophan, obtained by FT-ICR MS (colour code: CHON *vs.* CHO compounds). Inset pie charts show the fractions of compounds (CHO and CHON), identified by *Xc* values (●: $Xc < 2.50$; ●: $2.50 \leq Xc < 2.71$; ●: $Xc \geq 2.71$). **(b)** Time evolution of the absorption spectrum of 0.1 mM tryptophan during the irradiation experiments (measured over a 1 cm optical path length, after 1:3 dilution with 10 mM phosphate buffer at pH 7). Values of the spectral slope *S*, calculated in the wavelength interval of 290–310 nm, are also highlighted. (For interpretation of the references to colour in this figure legend, the reader is referred to the Web version of this article.)

changes (Fig. 8b), including the increase in long-wavelength (*i.e.*, >300 nm) absorbance and the decrease in *S* (Berto et al., 2018; Bianco et al., 2014; Jiang et al., 2021; Smith et al., 2016). Formation of compounds with higher molecular mass was also observed in the case of tyrosine irradiation (see Fig. S8 in SM). By comparing Fig. 8 with Fig. S8 (SM) one gets that fragmentation (formation of compounds with lower molecular mass) was comparatively more important for tryptophan than for tyrosine. However, tryptophan also produced a higher fraction of polyaromatic compounds.

Parallel increases in both absorbance and molecular mass upon irradiation have also been reported in the case of environmentally significant phenolic compounds, which are also known photochemical sources of HS-like substances (Smith et al., 2016; Vione et al., 2021; Tang et al., 2020). It is possible that such processes occur in at least some of the irradiated lake water samples, and account for similar effects on the absorption spectra.

In addition to direct irradiation of precursor molecules, formation of compounds with higher molecular mass might also take place in the presence of photochemically produced reactive intermediates, generated by irradiation of surface-water photosensitisers. For instance, dimerisation and oligomerisation of phenolic compounds is known to be induced by photogenerated carbonate radicals ($CO_3^{\bullet-}$) (Alvarez et al., 2007; Yan et al., 2019), and by excited triplet states that can be formed upon irradiation of chromophoric dissolved organic matter (Loiselle et al., 2009; De Laurentiis et al., 2013).

4. Conclusions

Here we provide evidence that irradiation is able to trigger significant formation of HS-like fluorescent compounds, in some water samples collected from mountain lakes in late summer. Fluorophore formation could be best highlighted in samples showing high initial values of protein-like vs. HS-like contribution ratios to fluorescence, as derived from PARAFAC analysis. In such samples, possible photobleaching of initially occurring HS-like fluorophores would have limited ability to interfere with photoinduced generation of further HS-like fluorescing compounds. Sample choice was probably important, as mountain lakes in late summer often show low intensity of HS-like fluorescence. While similar phenomena could also occur in lowland lake samples, they might be masked by photobleaching of existing HS.

Still, such processes might possibly be highlighted in protein-rich environments, irrespective of altitude (*e.g.* lakes during, or soon after, algal blooms).

Fluorescence increase in the humic region took place alongside with an increase in sample absorbance (which is the opposite to photobleaching) and, sometimes, a decrease in spectral slope. These phenomena increase radiation absorption by lake water at higher wavelengths, which has potential ecologic significance because radiation-absorbing compounds screen biologically harmful UV radiation. Therefore, photoinduced chromophore formation in otherwise clear water environments might play a role in decreasing UV stress to living organisms. The interplay between chromophore photogeneration and photobleaching (likely taking place at the same time) will require further investigation.

Photochemical formation of HS-like fluorophores would be an autochthonous (in-lake) process. Humic compounds occurring in natural waters derive in large part from terrestrial sources (Stedmon et al., 2003) and they are often taken as markers of allochthonous organic matter. Therefore, the processes studied in this work might potentially introduce a bias in source apportionment of organic matter, in particular in those aquatic environments where photochemistry plays an important role as source of HS-like fluorophores. The possibility that at least a fraction of HS may be autochthonous in origin is currently (or should be) taken into account (Yang et al., 2021).

The origin of the fluorescence increase will also require further investigation. Photochemical precursors (tyrosine, tryptophan, and several phenols) of HS-like substances are all able to produce compounds with higher molecular mass when irradiated, which also leads to an increase in long-wavelength absorbance. Such a scenario, though reasonable, still has to be conclusively demonstrated. For instance, although the precursor molecules have been irradiated in ultra-pure water (both here and in previous works), they have not been spiked to natural water samples under irradiation, which would provide a further test of their potential to act as HS-like precursors.

Credit author statement

Luca Carena: Investigation; Formal analysis; Data curation; Writing – review & editing. Yiqun Wang: Investigation; Validation; Data curation; Writing – original draft. Sasho Gligorovski: Resources, Supervision; Validation; Writing – review & editing. Silvia Berto: Resources, Supervision; Validation; Writing – review & editing. Stéphane Mounier: Validation; Data curation; Writing – review & editing. Davide Vione: Conceptualization; Supervision; Validation; Writing – original draft; Writing – review & editing.

Declaration of competing interest

The authors declare that they have no known competing financial interests or personal relationships that could have appeared to influence the work reported in this paper.

Data availability

Data will be made available on request.

Acknowledgements

L.C. and D.V. wish to thank Dr. S. Bertinetti and Mr. L. Rapa for their help during lake-water sampling. L.C. acknowledges Compagnia di San Paolo (Torino, Italy) for financially supporting his PhD fellowship. The stay of D.V. in Toulon was financially supported by invited research call 2021.

Appendix A. Supplementary data

Supplementary data to this article can be found online at https://doi.org/10.1016/j.chemosphere.2023.137972.

References

Alvarez, M.N., Peluffo, G., Folkes, L., Wardman, P., Radi, R., 2007. Reaction of the carbonate radical with the spin-trap 5,5-dimethyl-1-pyrroline-N-oxide in chemical and cellular systems: pulse radiolysis, electron paramagnetic resonance, and kinetic-competition studies. Free Radical Biol. Med. 43, 1523–1533. https://doi.org/10.1016/j.freeradbiomed.2007.08.002.

Andersen, C.M., Bro, R., 2003. Practical aspects of PARAFAC modeling of fluorescence excitation-emission data. J. Chemom. 17, 200–215. https://doi.org/10.1002/cem.790.

Berg, S.M., Whiting, Q.T., Herrli, J.A., Winkels, R., Wammer, K.H., Remucal, C.K., 2019. The role of dissolved organic matter composition in determining photochemical reactivity at the molecular level. Environ. Sci. Technol. 53, 11725–11734. https://doi.org/10.1021/acs.est.9b03007.

Berto, S., De Laurentiis, E., Scapuzzi, C., Chiavazza, E., Corazzari, I., Turci, F., Minella, M., Buscaino, R., Daniele, P.G., Vione, D., 2018. Phototransformation of l-tryptophan and formation of humic substances in water. Environ. Chem. Lett. 16, 1035–1041. https://doi.org/10.1007/s10311-018-0714-y.

Berto, S., De Laurentiis, E., Tota, T., Chiavazza, E., Daniele, P.G., Minella, M., Isaia, M., Brigante, M., Vione, D., 2016. Properties of the humic-like material arising from the photo-transformation of l-tyrosine. Sci. Total Environ. 545 (546), 434–444. https://doi.org/10.1016/j.scitotenv.2015.12.047.

Bianco, A., Minella, M., De Laurentiis, E., Maurino, V., Minero, C., Vione, D., 2014. Photochemical generation of photoactive compounds with fulvic-like and humic-like fluorescence in aqueous solution. Chemosphere 111, 529–536. https://doi.org/10.1016/j.chemosphere.2014.04.035.

Bridgeman, J., Bieroza, M., Baker, A., 2011. The application of fluorescence spectroscopy to organic matter characterisation in drinking water treatment. Rev. Environ. Sci. Bio/Technology 10, 277. https://doi.org/10.1007/s11157-011-9243-x.

Brinkmann, T., Sartorius, D., Frimmel, F.H., 2003. Photobleaching of humic rich dissolved organic matter. Aquat. Sci. 65, 415–424. https://doi.org/10.1007/s00027-003-0670-9.

Bro, R., 1997. PARAFAC. Tutorial and applications. Chemometr. Intell. Lab. Syst. 38, 149–171. https://doi.org/10.1016/S0169-7439(97)00032-4.

Carena, L., Puscasu, C.G., Comis, S., Sarakha, M., Vione, D., 2019. Environmental photodegradation of emerging contaminants: a re-examination of the importance of triplet-sensitised processes, based on the use of 4-carboxybenzophenone as proxy for the chromophoric dissolved organic matter. Chemosphere 237, 124476. https://doi.org/10.1016/j.chemosphere.2019.124476.

Clark, J.B., Neale, P., Tzortziou, M., Cao, F., Hood, R.R., 2019. A mechanistic model of photochemical transformation and degradation of colored dissolved organic matter. Mar. Chem. 214, 103666 https://doi.org/10.1016/j.marchem.2019.103666.

Coble, P.G., 1996. Characterization of marine and terrestrial DOM in seawater using excitation-emission matrix spectroscopy. Mar. Chem. 51, 325–346. https://doi.org/10.1016/0304-4203(95)00062-3.

Cory, R.M., McKnight, D.M., 2005. Fluorescence spectroscopy reveals ubiquitous presence of oxidized and reduced quinones in dissolved organic matter. Environ. Sci. Technol. 39, 8142–8149. https://doi.org/10.1021/es0506962.

Dainard, P.G., Gueguen, C., McDonald, N., Williams, W.J., 2015. Photobleaching of fluorescent dissolved organic matter in beaufort sea and north atlantic subtropical gyre. Mar. Chem. 177, 630–637. https://doi.org/10.1016/j.marchem.2015.10.004.

De Laurentiis, E., Minella, M., Maurino, V., Minero, C., Brigante, M., Mailhot, G., Vione, D., 2012. Photochemical production of organic matter triplet states in water samples from mountain lakes, located below or above the tree line. Chemosphere 88, 1208–1213. https://doi.org/10.1016/j.chemosphere.2012.03.071.

De Laurentiis, E., Sur, B., Pazzi, M., Maurino, V., Minero, C., Mailhot, G., Brigante, M., Vione, D., 2013. Phenol transformation and dimerisation, photosensitised by the triplet state of 1-nitronaphthalene: a possible pathway to humic-like substances (HULIS) in atmospheric waters. Atmos. Environ. 70, 318–327. https://doi.org/10.1016/j.atmosenv.2013.01.014.

De Paolis, F., Kukkonen, J., 1997. Binding of organic pollutants to humic and fulvic acids: influence of pH and the structure of humic material. Chemosphere 34, 1693–1704. https://doi.org/10.1016/S0045-6535(97)00026-X.

Del Vecchio, R., Blough, N.V., 2002. Photobleaching of chromophoric dissolved organic matter in natural waters: kinetics and modeling. Mar. Chem. 78, 231–253. https://doi.org/10.1016/S0304-4203(02)00036-1.

Fox, B.G., Thorn, R.M.S., Anesio, A.M., Cox, T., Attridge, J.W., Reynolds, D.M., 2019. Microbial Processing and Production of Aquatic Fluorescent Organic Matter in a Model Freshwater System. Water. https://doi.org/10.3390/w11010010.

Fox, B.G., Thorn, R.M.S., Anesio, A.M., Reynolds, D.M., 2017. The in situ bacterial production of fluorescent organic matter; an investigation at a species level. Water Res. 125, 350–359. https://doi.org/10.1016/j.watres.2017.08.040.

Galbavy, E.S., Ram, K., Anastasio, C., 2010. Chemistry 2-Nitrobenzaldehyde as a chemical actinometer for solution and ice photochemistry. J. Photochem. Photobiol. Chem. 209, 186–192. https://doi.org/10.1016/j.jphotochem.2009.11.013.

Galgani, L., Tognazzi, A., Rossi, C., Ricci, M., Angel Galvez, J., Dattilo, A.M., Cozar, A., Bracchini, L., Loiselle, S.A., 2011. Assessing the optical changes in dissolved organic matter in humic lakes by spectral slope distributions. J. Photochem. Photobiol. B Biol. 102, 132–139. https://doi.org/10.1016/j.jphotobiol.2010.10.001.

Gu, Y., , Lensu, A., Perämäki, S., Ojala, A., Vähätalo, A. V, 2017. Iron and pH regulating the photochemical mineralization of dissolved organic carbon. ACS Omega 2, 1905–1914. https://doi.org/10.1021/acsomega.7b00453.

He, W., Choi, I., Lee, J.-J., Hur, J., 2016. Coupling effects of abiotic and biotic factors on molecular composition of dissolved organic matter in a freshwater wetland. Sci. Total Environ. 544, 525–534. https://doi.org/10.1016/j.scitotenv.2015.12.008.

Helms, J.R., Mao, J., Stubbins, A., Schmidt-Rohr, K., Spencer, R.G.M., Hernes, P.J., Mopper, K., 2014. Loss of optical and molecular indicators of terrigenous dissolved organic matter during long-term photobleaching. Aquat. Sci. 76, 353–373. https://doi.org/10.1007/s00027-014-0340-0.

Helms, J.R., Stubbins, A., Ritchie, J.D., Minor, E.C., Kieber, D.J., Mopper, K., 2008. Absorption spectral slopes and slope ratios as indicators of molecular weight, source, and photobleaching of chromophoric dissolved organic matter. Limnol. Oceanogr. 53, 955–969. https://doi.org/10.4319/lo.2008.53.3.0955.

Hoffer, A., Kiss, G., Blazsó, M., Gelencsér, A., 2004. Chemical characterization of humic-like substances (HULIS) formed from a lignin-type precursor in model cloud water. Geophys. Res. Lett. 31 https://doi.org/10.1029/2003GL018962.

Jiang, W., Misovich, M.V., Hettiyadura, A.P.S., Laskin, A., McFall, A.S., Anastasio, C., Zhang, Q., 2021. Photosensitized reactions of a phenolic carbonyl from wood combustion in the aqueous phase—chemical evolution and light absorption properties of AqSOA. Environ. Sci. Technol. 55, 5199–5211. https://doi.org/10.1021/acs.est.0c07581.

Koukal, B., , Guéguen, C., Pardos, M., Dominik, J., 2003. Influence of humic substances on the toxic effects of cadmium and zinc to the green alga Pseudokirchneriella subcapitata. Chemosphere 53, 953–961. https://doi.org/10.1016/S0045-6535(03)00720-3.

Kourtchev, I., Godoi, R.H.M., Connors, S., Levine, J.G., Archibald, A.T., Godoi, A.F.L., Paralovo, S.L., Barbosa, C.G.G., Souza, R.A.F., Manzi, A.O., Seco, R., Sjostedt, S., Park, J.-H., Guenther, A., Kim, S., Smith, J., Martin, S.T., Kalberer, M., 2016. Molecular composition of organic aerosols in central Amazonia: an ultra-high-resolution mass spectrometry study. Atmos. Chem. Phys. 16, 11899–11913. https://doi.org/10.5194/acp-16-11899-2016.

Krachler, R., Krachler, R.F., 2021. Northern high-latitude organic soils as a vital source of river-borne dissolved iron to the ocean. Environ. Sci. Technol. 55, 9672–9690. https://doi.org/10.1021/acs.est.1c01439.

Liu, Y., Mekic, M., Carena, L., Vione, D., Gligorovski, S., Zhang, G., Jin, B., 2020. Tracking photodegradation products and bond-cleavage reaction pathways of triclosan using ultra-high resolution mass spectrometry and stable carbon isotope analysis. Environ. Pollut. 264, 114673 https://doi.org/10.1016/j.envpol.2020.114673.

Loisel, G., Mekic, M., Liu, S., Song, W., Jiang, B., Wang, Y., Deng, H., Gligorovski, S., 2021. Ionic strength effect on the formation of organonitrate compounds through photochemical degradation of vanillin in liquid water of aerosols. Atmos. Environ. 246, 118140 https://doi.org/10.1016/j.atmosenv.2020.118140.

Loiselle, S.A., Bracchini, L., Dattilo, A.M., Ricci, M., Tognazzi, A., , Cózar, A., Rossi, C., 2009. The optical characterization of chromophoric dissolved organic matter using wavelength distribution of absorption spectral slopes. Limnol. Oceanogr. 54, 590–597. https://doi.org/10.4319/lo.2009.54.2.0590.

Mabato, B.R.G., Lyu, Y., Ji, Y., Li, Y.J., Huang, D.D., Li, X., Nah, T., Lam, C.H., Chan, C. K., 2022. Aqueous secondary organic aerosol formation from the direct photosensitized oxidation of vanillin in the absence and presence of ammonium nitrate. Atmos. Chem. Phys. 22, 273–293. https://doi.org/10.5194/acp-22-273-2022.

Mekic, M., Zeng, J., Jiang, B., Li, X., Lazarou, Y.G., Brigante, M., Herrmann, H., Gligorovski, S., 2020. Formation of toxic unsaturated multifunctional and organosulfur compounds from the photosensitized processing of fluorene and DMSO at the air-water interface. J. Geophys. Res. Atmos. 125, e2019JD031839 https://doi.org/10.1029/2019JD031839.

Minor, E.C., Swenson, M.M., Mattson, B.M., Oyler, A.R., 2014. Structural characterization of dissolved organic matter: a review of current techniques for isolation and analysis. Environ. Sci. Process. Impacts 16, 2064–2079. https://doi.org/10.1039/C4EM00062E.

Murphy, K.R., Stedmon, C.A., Graeber, D., Bro, R., 2013. Fluorescence spectroscopy and multi-way techniques. PARAFAC. Anal. Methods 5, 6557–6566. https://doi.org/10.1039/C3AY41160E.

Nelson, N.B., Siegel, D.A., 2013. The global distribution and dynamics of chromophoric dissolved organic matter. Ann. Rev. Mar. Sci 5, 447–476. https://doi.org/10.1146/annurev-marine-120710-100751.

Nguyen, H.V.-M., Lee, M.-H., Hur, J., Schlautman, M.A., 2013. Variations in spectroscopic characteristics and disinfection byproduct formation potentials of dissolved organic matter for two contrasting storm events. J. Hydrol. 481, 132–142. https://doi.org/10.1016/j.jhydrol.2012.12.044.

Niu, X.-Z., Liu, C., Gutierrez, L., Croué, J.-P., 2014. Photobleaching-induced changes in photosensitizing properties of dissolved organic matter. Water Res. 66, 140–148. https://doi.org/10.1016/j.watres.2014.08.017.

Osburn, C.L., Stedmon, C.A., 2011. Linking the chemical and optical properties of dissolved organic matter in the Baltic–North Sea transition zone to differentiate three allochthonous inputs. Mar. Chem. 126, 281–294. https://doi.org/10.1016/j.marchem.2011.06.007.

Remucal, C.K., 2014. The role of indirect photochemical degradation in the environmental fate of pesticides: a review. Environ. Sci. Process. Impacts 16, 628–653. https://doi.org/10.1039/c3em00549f.

Shank, G.C., Zepp, R.G., , Vähätalo, A., Lee, R., Bartels, E., 2010. Photobleaching kinetics of chromophoric dissolved organic matter derived from mangrove leaf litter and floating Sargassum colonies. Mar. Chem. 119, 162–171. https://doi.org/10.1016/j.marchem.2010.01.003.

Sharpless, C.M., Blough, N.V., 2014. The importance of charge-transfer interactions in determining chromophoric dissolved organic matter (CDOM) optical and photochemical properties. Environ. Sci. Process. Impacts 16, 654–671. https://doi.org/10.1039/c3em00573a.

Smith, J.D., Kinney, H., Anastasio, C., 2016. Phenolic carbonyls undergo rapid aqueous photodegradation to form low-volatility, light-absorbing products. Atmos. Environ. 126, 36–44. https://doi.org/10.1016/j.atmosenv.2015.11.035.

Sommaruga, R., 2001. The role of solar UV radiation in the ecology of alpine lakes. J. Photochem. Photobiol. B Biol. 62, 35–42. https://doi.org/10.1016/S1011-1344(01)00154-3.

Sommaruga, R., Psenner, R., Schafferer, E., Koinig, K.A., Sommaruga-Wögrath, S., 1999. Dissolved organic carbon concentration and phytoplankton biomass in high-mountain lakes of the Austrian Alps: potential effect of climatic warming on UV underwater attenuation. Arctic Antarct. Alpine Res. 31, 247–253. https://doi.org/10.1080/15230430.1999.12003305.

Stedmon, C.A., Markager, S., Bro, R., 2003. Tracing dissolved organic matter in aquatic environments using a new approach to fluorescence spectroscopy. Mar. Chem. 82, 239–254. https://doi.org/10.1016/S0304-4203(03)00072-0.

Suzuki, D., Shoji, R., 2020. Toxicological effects of chlorophenols to green algae observed at various pH and concentration of humic acid. J. Hazard Mater. 400, 123079 https://doi.org/10.1016/j.jhazmat.2020.123079.

Tang, S., Li, F., Tsona, N.T., Lu, C., Wang, X., Du, L., 2020. Aqueous-phase photooxidation of vanillic acid: a potential source of humic-like substances (HULIS). ACS Earth Sp. Chem. 4, 862–872. https://doi.org/10.1021/acsearthspacechem.0c00070.

Tipping, E., Woof, C., Rigg, E., Harrison, A.F., Ineson, P., Taylor, K., Benham, D., Poskitt, J., Rowland, A.P., Bol, R., Harkness, D.D., 1999. Climatic influences on the leaching of dissolved organic matter from upland UK moorland soils, investigated by a field manipulation experiment. Environ. Int. 25, 83–95. https://doi.org/10.1016/S0160-4120(98)00098-1.

Trubetskaya, O.E., Richard, C., Trubetskoj, O.A., 2016. High amounts of free aromatic amino acids in the protein-like fluorescence of water-dissolved organic matter. Environ. Chem. Lett. 14, 495–500. https://doi.org/10.1007/s10311-016-0556-4.

Vähätalo, A. V, Wetzel, R.G., 2004. Photochemical and microbial decomposition of chromophoric dissolved organic matter during long (months–years) exposures. Mar. Chem. 89, 313–326. https://doi.org/10.1016/j.marchem.2004.03.010.

Vione, D., Minella, M., Maurino, V., Minero, C., 2014. Indirect photochemistry in sunlit surface waters: photoinduced production of reactive transient species. Chem. Eur J. 20, 10590–10606. https://doi.org/10.1002/chem.201400413.

Vione, D., Minero, C., Carena, L., 2021. Fluorophores in surface freshwaters: importance, likely structures, and possible impacts of climate change. Environ. Sci. Process. Impacts 23, 1429–1442. https://doi.org/10.1039/D1EM00273B.

Wang, Y., Deng, H., Li, P., Xu, J., Jiang, B., Pang, H., Gligorovski, S., 2022a. Molecular Characterization of the product compounds formed upon heterogeneous chemistry of ozone with riverine surface microlayer. J. Geophys. Res. Atmos. 127, e2022JD037182 https://doi.org/10.1029/2022JD037182.

Wang, Y., Deng, H., Li, P., Xu, J., Loisel, G., Pang, H., Xu, X., Li, X., Gligorovski, S., 2022b. Interfacial ozone oxidation chemistry at a riverine surface microlayer as a source of nitrogen organic compounds. Environ. Sci. Technol. Lett. 9, 493–500. https://doi.org/10.1021/acs.estlett.2c00130.

Wang, Y., Mekic, M., Li, P., Deng, H., Liu, S., Jiang, B., Jin, B., Vione, D., Gligorovski, S., 2021. Ionic strength effect triggers brown carbon formation through heterogeneous ozone processing of ortho-vanillin. Environ. Sci. Technol. 55, 4553–4564. https://doi.org/10.1021/acs.est.1c00874.

Willett, K.L., Hites, R.A., 2000. Chemical actinometry : using o-nitrobenzaldehyde to measure light intensity in photochemical experiments. J. Chem. Educ. 77, 900–902. https://doi.org/10.1021/ed077p900.

Wolf, R., Thrane, J.-E., Hessen, D.O., Andersen, T., 2018. Modelling ROS formation in boreal lakes from interactions between dissolved organic matter and absorbed solar photon flux. Water Res. 132, 331–339. https://doi.org/10.1016/j.watres.2018.01.025.

Worms, I.A.M., Adenmatten, D., , Miéville, P., Traber, J., Slaveykova, V.I., 2015. Photo-transformation of pedogenic humic acid and consequences for Cd(II), Cu(II) and Pb (II) speciation and bioavailability to green microalga. Chemosphere 138, 908–915. https://doi.org/10.1016/j.chemosphere.2014.10.093.

Yamashita, Y., Nosaka, Y., Suzuki, K., Ogawa, H., Takahashi, K., Saito, H., 2013. Photobleaching as a factor controlling spectral characteristics of chromophoric dissolved organic matter in open ocean. Biogeosciences 10, 7207–7217. https://doi.org/10.5194/bg-10-7207-2013.

Yan, S., Liu, Y., Lian, L., Li, R., Ma, J., Zhou, H., Song, W., 2019. Photochemical formation of carbonate radical and its reaction with dissolved organic matters. Water Res. 161, 288–296. https://doi.org/10.1016/j.watres.2019.06.002.

Yang, X., Yuan, J., Yue, F.-J., Li, S.-L., Wang, B., Mohinuzzaman, M., Liu, Y., Senesi, N., Lao, X., Li, L., Liu, C.-Q., Ellam, R.M., Vione, D., Mostofa, K.M.G., 2021. New insights into mechanisms of sunlight- and dark-mediated high-temperature accelerated diurnal production-degradation of fluorescent DOM in lake waters. Sci. Total Environ. 760, 143377 https://doi.org/10.1016/j.scitotenv.2020.143377.

Yassine, M.M., Harir, M., Dabek-Zlotorzynska, E., Schmitt-Kopplin, P., 2014. Structural characterization of organic aerosol using Fourier transform ion cyclotron resonance

mass spectrometry: aromaticity equivalent approach. Rapid Commun. Mass Spectrom. 28, 2445–2454. https://doi.org/10.1002/rcm.7038.

Zepp, R.G., Sheldon, W.M., Moran, M.A., 2004. Dissolved organic fluorophores in southeastern US coastal waters: correction method for eliminating Rayleigh and Raman scattering peaks in excitation–emission matrices. Mar. Chem. 89, 15–36. https://doi.org/10.1016/j.marchem.2004.02.006.

Zhou, L., Sleiman, M., Fine, L., Ferronato, C., de Sainte Claire, P., Vulliet, E., Chovelon, J.-M., Xiu, G., Richard, C., 2019. Contrasting photoreactivity of β2-adrenoceptor agonists Salbutamol and Terbutaline in the presence of humic substances. Chemosphere 228, 9–16. https://doi.org/10.1016/j.chemosphere.2019.04.104.